Journal of Organometallic Chemistry 695 (2010) 1618–1626

Contents lists available at ScienceDirect

Journal of Organometallic Chemistry

journal homepage: www.elsevier.com/locate/jorganchem

Di-*n*-butyltin oxide as a chemical carbon dioxide capturer

Laurent Plasseraud [a], Danielle Ballivet-Tkatchenko [a], Hélène Cattey [a], Stéphane Chambrey [a], Rosane Ligabue [a], Philippe Richard [a], Rudolph Willem [b], Monique Biesemans [b,*]

[a] Institut de Chimie Moléculaire de l'Université de Bourgogne, UMR-CNRS 5260, Université de Bourgogne, 9 av A. Savary, F-21078 Dijon, France
[b] Vrije Universiteit Brussel (VUB), High Resolution NMR Centre (HNMR), Department of Materials and Chemistry (MACH), Pleinlaan 2, B-1050 Brussel, Belgium

ARTICLE INFO

Article history:
Received 23 February 2010
Received in revised form
8 April 2010
Accepted 15 April 2010
Available online 24 April 2010

Keywords:
Organotin(IV) oxide
Sn–O framework
2D heteronuclear correlation spectroscopy
Tin NMR
Crystal structure

ABSTRACT

Several synthetic routes to the decakis(di-*n*-butyltin(IV)) oxocluster, (n-$Bu_2SnO)_6[(n$-$Bu_2SnOCH_3)_2(CO_3)]_2$ (**1**), a diorganotin compound previously shown to belong to the class of organotins able to store carbon dioxide, as well as its reactivity toward dimethyl carbonate (DMC), are described. The synthetic route from n-Bu_2SnO and DMC was applied for the preparation of the ethoxy analogue of **1**, oxocluster **2**, using diethyl carbonate. The structural relationship connecting cluster **1**, with its precursor **PRE-1** isolated from recycling experiments and n-Bu_2SnO is discussed. For this purpose, the reactivity of **PRE-1** with trifluoromethanesulfonic acid was investigated in order to trace structural data. Solution and solid-state 1D NMR investigations of **1** and **2**, as well as $^1H-^{119}Sn$ 2D heteronuclear correlation spectroscopy experiments in solution, shed further insight into structural data.

1. Introduction

Organotin compounds with Sn–O bonds enjoy a large diversity of solid-state structures, from mononuclear compounds to complex clusters and multidimensional networks. Several reviews document their X-ray crystallographic structures [1]. In the growing field of metal-organic frameworks (MOFs), organotin(IV) carboxylates and dithiocarbamates can conveniently be used as building blocks for designing supramolecular architectures with large internal cavities [2]. In addition to their structural interest in its own, some organotin compounds display efficient catalytic activity. In particular, organotin triflates are used as catalysts for several organic reactions, such as the Mukaiyama aldol reaction [3], the Robinson annulation [4], the acetylation of alcohols [5] and transesterification reactions [6]. Furthermore, some organotin carboxylates are employed for industrial applications, for instance as stabilizers of poly(vinylchloride) and as catalysts for polyurethane synthesis and silicone vulcanisation [7]. In the challenging context of using CO_2 as renewable C_1 feed, it has been reported since two decades that organotin(IV) compounds can promote the direct carbonation of alcohols, which benefits from a CO_2 pressure increase [8]. In this context, some of us reported the facile CO_2 insertion into Sn–O bonds of a series of *n*-butyl(alkoxy)stannanes [9], and underlined the role of distannoxanes in the synthesis of dimethyl carbonate ($(CH_3O)_2CO$, DMC) from carbon dioxide [10]. X-ray structures of unprecedented isopropoxy stannane- and distannoxane-CO_2-adducts were unravelled [11]. Aiming at understanding these carbonation reaction mechanisms, we could isolate, during recycling experiments and after crystallisation from methanol at room temperature, single crystals of two organotin key intermediates exhibiting polynuclear frameworks and their crystal structure was analysed by X-ray diffraction (Fig. 1). In the *tert*-butyl series, a carbonato trinuclear oxocluster arrangement, [OC(OSn-*tert*-$Bu_2)_2O\cdot$*tert*-$Bu_2Sn(OH)_2$], was revealed [12], while in the case of the *n*-butyl analogue a novel decakis(diorganotin(IV)) oxocluster, (n-$Bu_2SnO)_6[(n$-$Bu_2SnOCH_3)_2(CO_3)]_2$ (**1**), was evidenced [13].

The present paper reports additional chemical properties on this fascinating class of organotin(IV) oxocluters, in particular, the optimisation of the synthesis of (n-$Bu_2SnO)_6[(n$-$Bu_2SnOCH_3)_2(CO_3)]_2$ (**1**) via organometallic routes, describes its reactivity toward organic carbonates, and explores its formation mechanism from di-*n*-butyltin oxide, n-Bu_2SnO. We investigated the structure of its original precursor, an amorphous material, hereafter **PRE-1**, collected during previous carbonation recycling experiments [13], and studied, in particular, the reactivity of **PRE-1** with trifluoromethanesulfonic acid (TfOH), allowing isolation of the trifluoromethanesulfonate organotin(IV) complex (**3**), of which we present the X-ray crystal structure. In addition, we present IR and NMR investigations of **1** and of the new compound **2**, the ethoxy analogue of **1**, (n-$Bu_2SnO)_6[(n$-$Bu_2SnOCH_2CH_3)_2(CO_3)]_2$, including

* Corresponding author. Tel.: +32 6293313; fax: +32 2 6293291.
E-mail address: mbiesema@vub.ac.be (M. Biesemans).

0022-328X/$ – see front matter © 2010 Elsevier B.V. All rights reserved.
doi:10.1016/j.jorganchem.2010.04.013

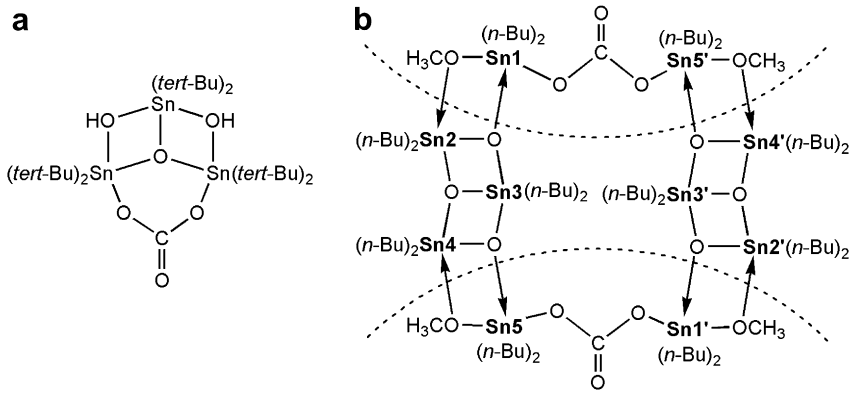

Fig. 1. Molecular representations of [OC(OSn-*tert*-Bu_2)$_2$O·*tert*-Bu_2Sn(OH)$_2$] (**a**) [11] and the decakis(diorganotin) oxocluster, (*n*-Bu_2SnO)$_6$[(*n*-Bu_2SnOCH$_3$)$_2$(CO_3)]$_2$ (compound **1**) (**b**) [12]. A formal partition of the molecular connectivity pattern of **1** into di-*n*-butyltin oxide moieties is given with the curved dotted lines.

results from solid-state NMR measurements as well as 2D ^{1}H–^{13}C and ^{1}H–^{119}Sn heteronuclear correlation spectroscopy experiments. Actually, it is shown that di-*n*-butyltin oxide acts as an efficient chemical CO_2 capturer.

2. Results and discussion

2.1. Syntheses

2.1.1. Synthetic routes to (*n*-$Bu_2SnO)_6$[(*n*-$Bu_2SnOCH_3)_2(CO_3)]_2$ (**1**)

As mentioned above, the decakis(diorganotin(IV)) oxocluster (*n*-$Bu_2SnO)_6$[(*n*-$Bu_2SnOCH_3)_2(CO_3)]_2$ (**1**) was originally isolated from a tin containing residue (**PRE-1**) collected after catalytic recycling experiments. X-ray crystallographic investigations revealed that **1** contains ten five-coordinate tin atoms with a distorted trigonal-bipyramidal configuration [13]. Its unexpected framework can be viewed as a pair of coplanar, pentameric (*n*-$Bu_2SnO)_5$ ladders bridged at their ends by two carbonate groups acting as μ_1,μ_1-bridging ligands and stabilized by four μ_2-bridging methoxy groups completing the five-coordinated configuration of the four tin atoms bound to the carbonate moieties. Complex **1** was synthesised via two synthetic pathways, one starting from di-*n*-butyltin oxide, *n*-Bu_2SnO, in a sealed vial (Scheme 1, pathway (iii)), the other starting from a chlorinated organotin precursor, *n*-$Bu_2Sn(OCH_3)Cl$ generated *in situ* from *n*-$Bu_2Sn(OCH_3)_2$ and *n*-Bu_2SnCl_2 (Scheme 1, pathway (iv)).

2.1.1.1. Preparation from n-Bu_2SnO and DMC in sealed vial. An equimolar mixture of *n*-Bu_2SnO and dimethyl carbonate in toluene, in the presence of methanol, and in sealed vial conditions reacted to a fine white powder, obtained after several washings with aliquots of methanol, and characterized as the oxocluster **1**, (*n*-$Bu_2SnO)_6$[(*n*-$Bu_2SnOCH_3)_2(CO_3)]_2$ from its three characteristic ^{119}Sn{^{1}H} resonances at δ −173, −177, and −234 ppm (C_6D_6, 298 K), in integrated area ratio 1:2:2, its two characteristic CO_3 stretching bands at 1539 and 1373 cm^{-1}, and its CH methoxy one at 2801 cm^{-1} (Fig. 2(a)) [13]. The yield in **1** could be optimised up to 80% (50% under with reflux conditions). IR and ^{119}Sn{^{1}H} NMR data achieved on the methanol wash fractions evidenced the exclusive presence of 1,3-dimethoxy-1,1,3,3-tetra-*n*-butyldistannoxane, {[*n*-$Bu_2(CH_3O)Sn]_2O\}_2$ (^{119}Sn{^{1}H} NMR ($CDCl_3$): δ −174, −181 ppm; IR 1062, 596 cm^{-1}) [10]. A much longer reaction time (overnight, 16 h) gives rise, in addition to {[*n*-$Bu_2(CH_3O)Sn]_2O\}_2$, also to its CO_2-adduct, 1-methoxy-3-methylcarbonato-1,1,3,3-tetra-*n*-butyldistannoxane, [*n*-$Bu_2(CH_3O)Sn]O[Sn(OC(O)OCH_3)$*n*-$Bu_2]$ (^{119}Sn{^{1}H} NMR ($CDCl_3$): δ −177, −208 ppm, IR: $\nu(CO_3)$ 1670 and 1300 cm^{-1})

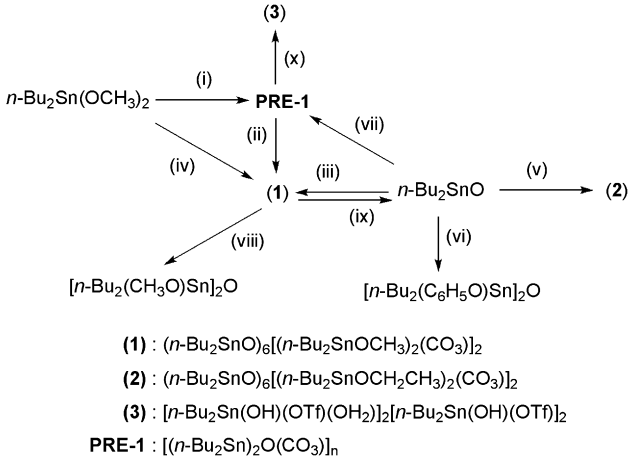

Scheme 1. Reactivity and relationship between *n*-Bu_2SnO, **1** and its precursor **PRE-1**. (i) methanol, carbon dioxide (423 K, 20 MPa). (ii) methanol (room temperature, several days). (iii) toluene, dimethyl carbonate, methanol (398 K, sealed vial), (iv) *n*-Bu_2SnCl_2, K_2CO_3, methanol (reflux), (v) toluene, diethyl carbonate, ethanol (398 K, sealed vial), (vi) toluene, diphenyl carbonate, phenol (398 K, sealed vial), (vii) toluene, carbon dioxide (383 K, 11 MPa), (viii) toluene, dimethyl carbonate (reflux), (ix) methanol, dimethyl carbonate (reflux), (x) TfOH (trifluoromethanesulfonic acid), acetonitrile (r.t.).

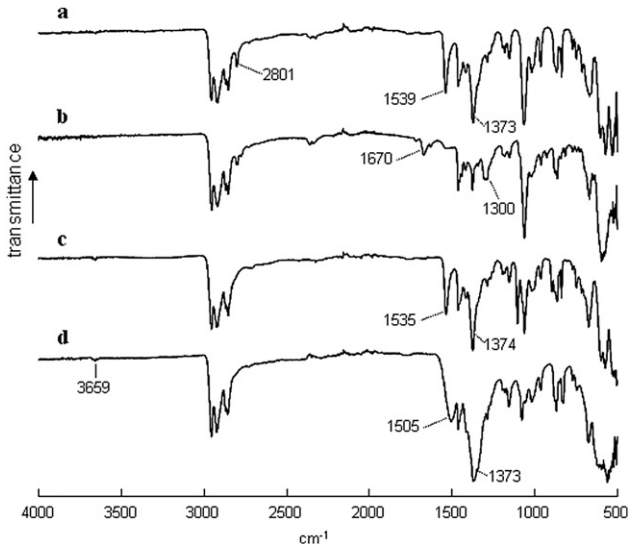

Fig. 2. IR(ATR) spectra of (a) **1**, (b) mixture of [*n*-$Bu_2(CH_3O)Sn]_2O$ and its CO_2-adduct, (c) **2**, and (d) **PRE-1**.

(Fig. 2(b)) [10], minor ^{119}Sn resonances characteristic for the decakis(diorganotin(IV)) oxocluster (**1**) being still observed. The formation of this CO_2-adduct can be explained by the decomposition of **1**, releasing CO_2, which then reacts with $\{[n\text{-}Bu_2(CH_3O)Sn]_2O\}_2$ leading to $[n\text{-}Bu_2(CH_3O)Sn]O[Sn(OC(O)OCH_3)n\text{-}Bu_2]$, since it was demonstrated previously that carbon dioxide inserts smoothly into the Sn–OR bond, giving a terminal alkylcarbonato fragment, –OC(O)OR [9, 11]. This is confirmed indirectly by the observation that under reflux, only the non-carbonated 1,3-dimethoxytetrabutyldistannoxane complex, $\{[n\text{-}Bu_2(CH_3O)Sn]_2O\}_2$, is generated. Therefore, it can be concluded that the decakis(diorganotin(IV)) oxocluster **1** constitutes a reaction intermediate, generated during the formation of 1,3-dimethoxy-1,1,3,3-tetra-*n*-butyldistannoxane from $n\text{-}Bu_2SnO$ and dimethyl carbonate. The oxocluster **1** can be described as a supramolecular construction consisting of two trinuclear $(n\text{-}Bu_2SnO)_3$ units and two $(n\text{-}Bu_2Sn OCH_3)_2(CO_3)$ fragments (see Fig. 1(b)), the former units being remnants of the polymeric structure of di-*n*-butyltin oxide as proposed by Harris and Sebald (Fig. 3) [14,15]. Davis et al. apparently isolated **1** as a by-product, but since they targeted the 1,3-dimethoxy-1,1,3,3-tetra-*n*-butyldistannoxane derivatives, no spectroscopic data on **1** were reported [16].

2.1.1.2. Isolation from n-Bu$_2$Sn(OCH$_3$)Cl and K$_2$CO$_3$ under reflux. The X-ray crystallographic analysis of oxocluster **1** as well as the construction mechanism proposed above support the involvement of the transient fragment, $(n\text{-}Bu_2SnOCH_3)_2(CO_3)$, probably reflecting DMC formation. Our second approach to mimic the synthetic reconstitution of **1** consisted in generating synthetically this functional unit by direct reaction between two equivalents of $n\text{-}Bu_2Sn(OCH_3)Cl$ and one equivalent of K_2CO_3 in methanol. Di-*n*-butylmethoxytin chloride, $n\text{-}Bu_2Sn(OCH_3)Cl$, preliminarily prepared by mixing equimolar amounts of di-*n*-butyltin dichloride and di-*n*-butyltin dimethoxide [17], was stirred and refluxed with K_2CO_3 in methanol for 2 h. After separation of the KCl precipitate, colourless crystals obtained as a by-product appeared to be **1**, as confirmed by $^{119}Sn\{^1H\}$, $^{13}C\{^1H\}$ NMR and IR spectra. Its yield did not exceed 10%, however, but the structure of the major organotin compound obtained as an oil could not be unravelled.

*2.1.2. Syntheses of (n-Bu$_2$SnO)$_6$[(n-Bu$_2$SnOCH$_2$CH$_3$)$_2$(CO$_3$)]$_2$(**2**) in sealed vial*

The synthesis of **1** from $n\text{-}Bu_2SnO$ and DMC in a sealed vial providing a satisfactory yield, higher than 80%, this synthetic method was applied to other organic carbonates in order to generate other oxocluster analogues of **1**. Application to $n\text{-}Bu_2SnO$, diethyl carbonate, and ethanol in toluene under similar conditions as for **1** (see experimental Section 4.3) provided the new carbonato compound **2** which is less soluble in organic solvents and more sensitive to air than **1**. Its $^{119}Sn\{^1H\}$ NMR pattern in C_6D_6 is similar to **1**, with again three signals, at δ –173, –178 and –234 ppm in area ratio 1:2:2. The solution ^1H and $^{13}C\{^1H\}$ NMR spectra confirmed the complete analogy between **1** and **2** (see Section 2.2).

By contrast, applying the same procedure with diphenyl carbonate, $(C_6H_5O)_2CO$, did not result in the expected phenoxy decakis(diorganotin) analogue of **1**. Thus, the $^{119}Sn\{^1H\}$ NMR (298 K) spectrum in $CDCl_3$ exhibits only a single pair of signals at δ –176 and –177 ppm and no IR bands characteristic for a carbonato function were observed. By comparison with NMR and IR data from previous data [18,19], the compound obtained quantitatively appears to be 1,3-diphenoxy-1,1,3,3-tetra-*n*-butyldistannoxane, $\{[n\text{-}Bu_2(C_6H_5O)Sn]_2O\}_2$ (Fig. 4).

2.1.3. Preparation and basic characterization of PRE-1

Initially, the formation of a white powder, hereafter **PRE-1**, was observed when a methanol solution of $n\text{-}Bu_2Sn(OCH_3)_2$ (0.2 M) was exposed to 20 MPa of CO_2 for 15 h at 423 K, under supercritical conditions, followed by elimination of methanol, dimethyl carbonate and water. The ES positive mode mass spectrum of the methanolic mother liquor, after preliminary distillation of volatile organics, exhibited four mass clusters at *m*/*z* 741.1 (100%), 1011.1 (29%), 1245.1 (35%), 1493.2 (6%) that can be assigned to di-*n*-butyltin oxide-based oligomeric species, $[(C_4H_9)_2SnO]_n$, with three to six tin atoms, respectively. Interestingly, an additional *m*/*z* value at 807.1 (17%), could correspond to a plausible, non-charged diprotonated carbonato trinuclear species with formula $[((C_4H_9)_2SnO)_3(CO_3)H_2]$ and molar mass 808.94, from which one electron is ejected in the mass spectrometer to the fragment $[((C_4H_9)_2SnO)_3(CO_3)H_2]^+$. This trinuclear species is the analogue of the compound isolated in the *tert*-butyl series (Fig. 1 [12](a)), and reflecting effectively chemical CO_2 capture.

Once isolated in powder form, **PRE-1** displayed IR bands (Fig. 2(d)) characteristic for neither the starting $n\text{-}Bu_2Sn(OCH_3)_2$ nor di-*n*-butyltin oxide, $n\text{-}Bu_2SnO$. **PRE-1** is an amorphous material, air-stable, insoluble in most organic solvents, but still active in supercritical CO_2 for DMC formation upon multi-fold recycling [13]. The IR spectra of the residue recorded after each catalytic run were identical, supporting the presence of a single organotin compound. **PRE-1** was also obtained from $n\text{-}Bu_2SnO$ and supercritical CO_2 without any presence of methanol. Being highly insoluble, no solution NMR spectra of **PRE-1** could be recorded. **PRE-1** displays two strong stretching bands absorptions at 1505 and 1373 cm^{-1}, characteristic for a carbonate function (Fig. 2(d)). However, these two bands are broader than in **1** and **2**, suggesting that possibly two or even more carbonate functions with slightly different chemical environments might be present. In 1983, Smith and Hill reported the preparation and ^{119}Sn Mössbauer and IR studies of a series of hydrated diorganotin oxycarbonates of the type $(R_2Sn)_2OCO_3\cdot nH_2O$ (R = Me, Et, Ph, $n = 0$; R = Pr, Bu, Oct, $n = 1$), obtained from an equimolar mixture of diorganotin dichloride and cesium carbonate at room temperature [20]. Interestingly, these compounds are also reported to be insoluble and to display IR low frequency, carbonyl stretching bands in the range 1495–1515 cm^{-1}. The structure proposed from work of Goel and coworkers [21], consisted of a polymeric framework containing intermolecularly bridging carbonate groups and four-membered Sn_2O_2 rings (Fig. 5(a)). In view of their non-solubility and

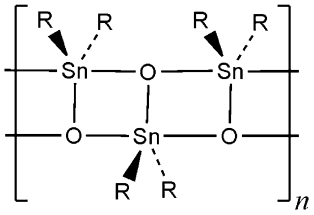

Fig. 3. Linear, ladder-type, polymeric structure construction for R_2SnO (R = *n*-Bu), as proposed by Harris and Sebald [14].

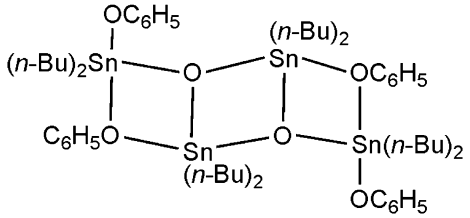

Fig. 4. Dimeric, ladder-type structure of $[n\text{-}Bu_2(C_6H_5O)Sn]_2O$.

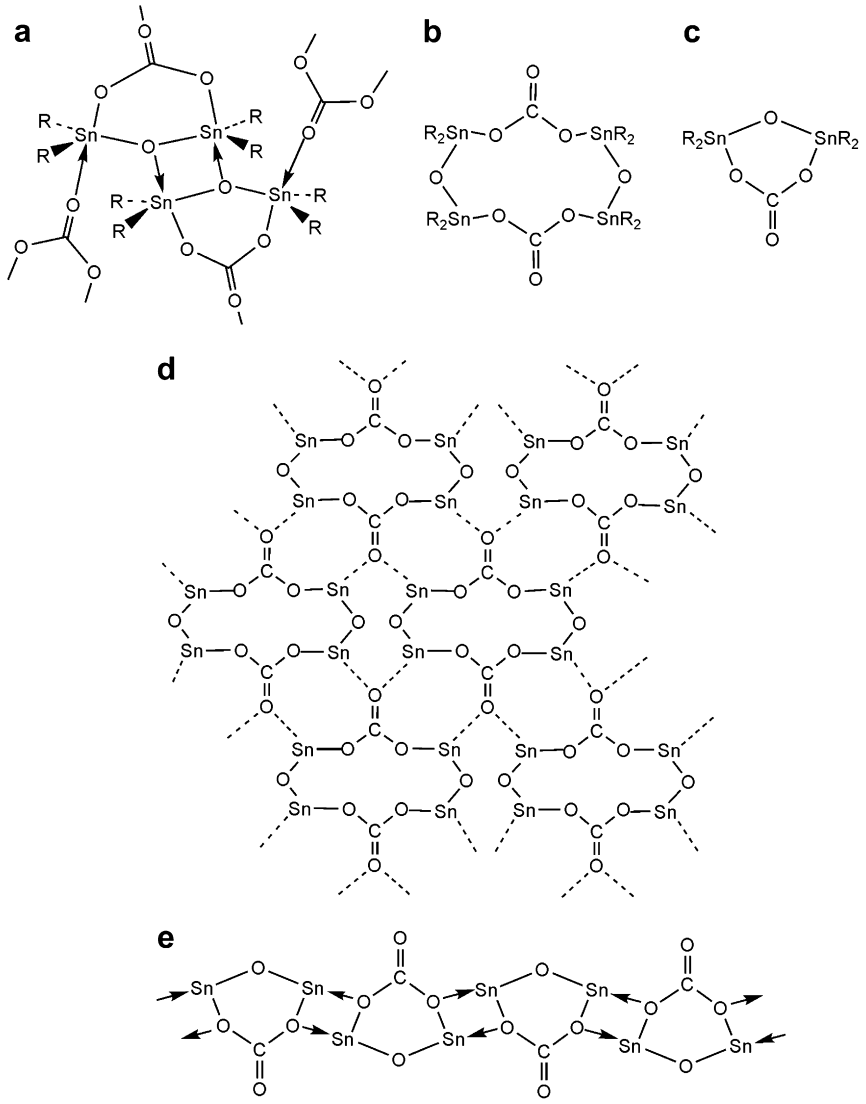

Fig. 5. Possible structures for **PRE-1,** (**a**) based on the Goel's model [20], (**b**) basic motif derived from the decanuclear framework of **1**, (**c**) basic structural unit for framework in (**a**), (**d**) proposed cross-linked network based on structural motif (**b**), (**e**) proposed cross-linked network based on structural motif (**c**).

IR data, the similarity between the precursor **PRE-1** and the diorganotin oxycarbonate $(n\text{-}Bu_2Sn)_2OCO_3\cdot H_2O$ described by Smith and Hill [20] is significant. Furthermore, the similar elemental compositions found for **PRE-1** [C = 38.76, H = 7.12, Sn = 44.93] and $(n\text{-}Bu_2Sn)_2OCO_3\cdot H_2O$ [C = 36.46, H = 6.85, Sn = 42.40] [20] likewise supports this analogy, even though the empirical formula 2 $(Bu_2SnO)CO_2$ [C = 37.67, H = 6.71, Sn = 43.81], which is merely dehydrated $(n\text{-}Bu_2Sn)_2OCO_3\cdot H_2O$, matches even better the experimental analysis data.

2.2. Multinuclear NMR investigation of *1* and *PRE-1*

Even though 1D ^1H, $^{13}C\{^1H\}$ and ^{119}Sn solution spectra of **1** reflect the features of **1** (Fig. 1(b)) [13], thus suggesting that the solid-state structure of **1** is retained in solution, the lack of detailed signal assignment prevented so far formal characterization of the solution structure of **1**. 2D $^1H-^{13}C$ HSQC and HMBC as well as $^1H-^{119}Sn$ HMQC NMR experiments, performed for compounds **1** and **2** in C_6D_6 solution, addressed this issue.

Three sets of butyl resonances were identified from the $^1H-^{13}C$ correlation spectra. The HSQC spectrum allowed finding the ^1J ($^1H-^{13}C$) connectivity between the narrow-ranged but well separated ^{13}C resonances and the correlated, strongly overlapping proton resonances. The relationship between the carbon atoms and the protons of neighbouring groups was established through $^{2/3}J$ ($^1H-^{13}C$) connectivities observed in the HMBC spectrum. The 2D $^1H-^{119}Sn$ HMQC spectra recorded with variable preparation times indicate that the two intense ^{119}Sn resonances of **1** at −177 and −234 ppm display a correlation with the methoxy proton resonance, while the third half intense one (−173 ppm) does not. The other correlations visualized the scalar couplings between the ^{119}Sn and the corresponding butyl proton resonances, completing the assignment. Tables 1 and 2 provide the complete NMR assignments for compounds **1** and **2** respectively. The ^2J ($^1H-^{119}Sn$) coupling constants being larger than the ^3J ($^1H-^{119}Sn$) ones in the butyl chains is unusual, since in most cases the inverse holds [22], but not unique, since also very similar ^2J ($^1H-^{119}Sn$) and ^3J ($^1H-^{119}Sn$) [23] coupling constants following the sequence as mentioned here [24] have been described.

Apart from the correlations between ^{119}Sn and the corresponding butyl proton resonances, correlations are also observed between the ^{119}Sn resonance at −177 ppm and the α proton

Table 1
Selected ^{1}H, ^{13}C and ^{119}Sn chemical shifts (in ppm) and coupling constants between brackets in Hz, for **1** in C_6D_6 solution.

	OCH_3			Butyl α		Butyl β		Butyl γ		Butyl δ	
^{119}Sn	^{13}C	^{1}H		^{13}C	^{1}H	^{13}C	^{1}H	^{13}C	^{1}H	^{13}C	^{1}H
−234 [106, 198][a]	51.1	3.30	[n.r.]	23.4 [681/651][b]	1.52 [83][c]–1.65	28.0	1.96 [69][c]	27.8	1.57	14.1	1.08
−177 [106, 240][a]			[13]	21.6 [619/591][b]	1.25 [76][c]	28.3	1.81 [56][c]	27.9	1.44	13.9	0.98
−173 [198, 204][a]				24.6 [642/614][b]	1.75 [78][c]	28.8	2.00 [58][c]	28.2	1.71	14.5	1.19

[a] ^{2}J (^{119}Sn–$^{119/117}Sn$) coupling constants as mentioned in Ref. [13] for a $CDCl_3$ solution.
[b] ^{1}J (^{13}C–$^{119/117}Sn$) coupling constants as mentioned in Ref. [13] for a $CDCl_3$ solution.
[c] $^{2,3}J$ (^{1}H–^{119}Sn) coupling constants as determined from cross sections in the 2D ^{1}H–^{119}Sn HMQC spectra.

resonance of the butyl groups on the two other tin atoms, thus proving the existence of a bridging ^{119}Sn–O–^{119}Sn scalar coupling pathway involving this tin atom and the other two. The ^{119}Sn resonance at −177 ppm is assigned to tin atoms Sn2/4 (Fig. 1(b)), on the basis of the similarity in chemical shift (−173 ppm) for the resonance with half relative intensity, which, accordingly, needs to be assigned to tin atom Sn3, this assignment being also in conformity with respectively the presence and the absence of ^{1}H–^{119}Sn correlation with the methoxy proton resonance. This leaves the ^{119}Sn chemical shift of −234 ppm, likewise correlated with the methoxy proton resonance for tin atoms Sn1/5, in accordance with the carbonate group to which it is bound exerting more shielding. Completely similar patterns are found for compounds **1** and **2**, confirming both have the same structure in solution. The similarity between this proposed solution structure and the X-ray crystal structure is provided by the ^{117}Sn [25] solid-state spectrum of **1**, revealing three ^{117}Sn resonances in a 2:2:1 ratio at −235, −181, −171 ppm, respectively (Table 3), in close agreement with its ^{119}Sn chemical shifts at −234, −177, −173 ppm in solution. The solid-state ^{117}Sn spectrum displays a broad anisotropy pattern with relatively sharp lines, typical for a crystalline material (Table 3). The larger anisotropy is observed for the Sn1/5 and Sn3 atoms at the inside of the decatin ring, where distortion of the trigonal pyramidal Sn atom is more substantial than for Sn2/4 at the outside of the ring. A polyhedron coordination view, displaying the geometrical arrangement of the distorted trigonal bipyramidal tin atoms, is shown in Fig. 6.

The ^{117}Sn solid-state spectrum of **PRE-1** displays also a large anisotropy pattern of spinning side bands with an isotropic chemical shift at −229 ppm (Table 3), and probably also a minor one at −301 ppm, even though the latter cannot be confirmed unambiguously, due to the noisy nature of all the lines that are very broad, as usual for amorphous materials like **PRE-1**. The isotropic chemical shift of −229 ppm, very similar to the one in the decatin species **1** (−234 ppm), is assigned to a carbonate bound tin atom, strongly evidencing the presence of this structural unit in **PRE-1**. The solid-state ^{13}C CP–MAS spectrum of **PRE-1** displays two broad carbonyl resonances in a 1/3 integral ratio at 163.0 and 160.3 ppm, respectively, whereas **1** has a single sharp resonance at 164.0 ppm. No ^{13}C resonances from any alkoxy group is visible in **PRE-1**, as expected, since it can also be generated directly from CO_2 and Bu_2SnO without any involvement of methanol.

In spite of the above wealth of spectral data concerning **PRE-1**, its structure remains ill understood. Only a number of firm features, converging to tentative proposals, can be provided. The absence of a clearly identifiable intense OH band in its IR spectrum definitely disfavours **PRE-1** to be the hydrated di-*n*-butyltin oxycarbonate ($(n\text{-}Bu_2Sn)_2OCO_3\cdot H_2O$, as described by Smith and Hill [20], since the very weak band at 3659 cm^{-1} cannot realistically account for any composition containing OH moieties in stoichiometric amount. It can at most be present as an impurity in **PRE-1**. Furthermore, the isotropic ^{117}Sn chemical shift at −229 ppm, very similar to the value of −234 ppm found for the Sn1 atom of **1** bearing the carbonate group, by contrast with the isotropic ^{117}Sn chemical shift at −177 ppm, found for Bu_2SnO and also in **1**, definitely favours the presence of a $(n\text{-}Bu_2SnO)_2(CO)$ moiety in **PRE-1** similar to that of **1** itself, suggesting that the tin atom must be likewise five-coordinate in **PRE-1**. The latter, conjugated to the high non-solubility and amorphous nature of **PRE-1**, are arguments favouring the interpretation that the main ^{117}Sn resonance at −229 ppm, and the main ^{13}C resonance around −160 ppm raise from a symmetrically unique five-coordinate tin atom bound to a carbonate group, involved in a cross-linking network. On the basis of literature data, a possibility is *a priori* the network given in Fig. 5(a), as proposed by Goel and coworkers [21], the basic construction unit of which is shown in Fig. 5(c). The cross-linked network of Fig. 5(a), however, is not compatible with the observation of the main single isotropic ^{117}Sn chemical shift found for **PRE-1** since the network of Fig. 5(a) would require two isotropic ^{117}Sn chemical shifts with equal integrated areas, contrary to experimental evidence.

On the other hand, the motifs (b) and (c) of Fig. 5, both formally obeying the empirical formula $\{(n\text{-}Bu_2SnO)_2(CO_2)\}_n$, with $n = 1$ for motif of Fig. 5(c) and $n = 2$ for motif of Fig. 5(b), match satisfactorily the elemental analysis data (see Section 2.1.3). We suggest that both the networks of Fig. 5(d) and (e) (where the two R groups have been omitted for clarity) might be the main cross-linked diorganotin motif of **PRE-1**, since both match all spectral data at hand, namely the single ^{117}Sn isotropic shift of −229 ppm very close to the one of **1** at −234 ppm, and that the ^{13}C NMR as well as the carbonyl IR data are also supporting it. The motif of Fig. 5(b) can be seen as that of **1**, from which the sequence $CH_3O\text{-}Sn_2(n\text{-}Bu)_2\text{-}O\text{-}Sn3(n\text{-}Bu)_2\text{-}O\text{-}Sn4(n\text{-}Bu)_2\text{-}OCH_3$ is removed, the Sn1 and Sn5 atoms of **1** being directly bridged by an O-atom in **PRE-1**. In this view, **PRE-1** is really a precursor of **1** in methanolic solution since **1** is merely **PRE-1**

Table 2
Selected ^{1}H, ^{13}C and ^{119}Sn chemical shifts (in ppm) and ^{n}J (^{1}H–$^{119/117}Sn$) coupling constants between brackets in Hz, for **2** in C_6D_6 solution.

	OCH_2			Butyl α		Butyl β		Butyl γ		Butyl δ	
^{119}Sn	^{13}C	^{1}H		^{13}C	^{1}H	^{13}C	^{1}H	^{13}C	^{1}H	^{13}C	^{1}H
−234 [112, 196][a]	58.9	3.59	[n.r.]	24.6	1.49 [88][c]–1.68	28.0	2.00 [65][c]	27.9	1.58	14.1	1.10
−178 [112, 240][a]			[18]	22.4 [681/651][b]	1.25 [79][c]	29.0	1.83 [54][c]	28.0	1.45	13.9	1.00
−173 [196][a]				24.6	1.77 [78][c]	28.9	2.01 [52][c]	28.3	1.72	14.6	1.21

[a] ^{2}J (^{119}Sn–$^{119/117}Sn$) coupling constants.
[b] ^{1}J (^{13}C–$^{119/117}Sn$) coupling constants.
[c] $^{2,3}J$ (^{1}H–^{119}Sn) coupling constants as determined from cross sections in the 2D ^{1}H–^{119}Sn HMQC spectra.

Table 3
Solution and solid-state tin NMR data.

Compound	δ (^{119}Sn)[a]	^{117}Sn MAS[b]					
		δ_{iso}	ζ	η	δ_{11}	δ_{22}	δ_{33}
1	−173 (20)	−174 (20)	−612	0.45	269	−6	−786
	−177 (40)	−181 (40)	−369	0.85	161	−153	−550
	−234 (40)	−235 (40)	−596	0.55	228	−101	−831
PRE-1	–	−227	−535	0.90	281	−200	−762

[a] In C_6D_6 solution. The numbers in parenthesis are the relative intensities of the resonances.

[b] δ_{iso} (ppm) = $(\delta_{11}+\delta_{22}+\delta_{33})/3$; ζ (ppm) = $\delta_{33} - \delta_{iso}$ and $\eta = |\delta_{22} - \delta_{11}|/|\delta_{33} - \delta_{iso}|$ were δ_{11}, δ_{22} and δ_{33} (ppm) are the principal tensor components of the chemical shielding anisotropy, sorted as follows $|\delta_{33} - \delta_{iso}| > |\delta_{11} - \delta_{iso}| > |\delta_{22} - \delta_{iso}|$.

stabilized by an additional pair of tetra-*n*-butyldimethoxydistannoxane molecules into each of which an additional *n*-Bu_2SnO unit is inserted. On the other hand, the amorphous **PRE-1** material must contain more than either single motif, given the probable presence of the additional resonance around −300 ppm in the solid-state ^{117}Sn spectrum, the unambiguous presence of two ^{13}C carbonyl resonances in ratio 1/3 in the solid-state ^{13}C NMR spectrum, and the significantly broader IR carbonyl bands of **PRE-1** (Fig. 2(d)) when compared to those of **1** (Fig. 2(a)). It is therefore proposed, without further firm evidence, on the basis of the data at hand, that **PRE-1** consists of a random mixture of at least two cross-linked motifs containing a five-coordinate tin atom bound to a single carbonate ligand, a major motif and a minor one. These motifs can be either of the two networks as discussed above, or even a different one, for instance a network of structural motifs 5(c) where each of the tin two atoms is interacting, as a Lewis acid, with the carbonyl oxygen atom of a neighbouring unit 5(c), acting as a Lewis base. However, given the limitation of the experimental data available for **PRE-1**, due to its high insolubility, and because also, unfortunately, so far, any attempts to isolate suitable single crystals of **PRE-1** failed, no structural feature can be discussed for **PRE-1**. An indirect attempt to shed some further light onto the actual framework structure of **PRE-1**, through a structure obtained from the reaction of **PRE-1** with trifluromethanesulfonate acid (TfOH), is presented in Section 2.3.2.

2.3. Reactivity

2.3.1. Reactivity of *1* toward DMC

In order to support experimentally our suggestion that oxocluster **1** constitutes a reaction intermediate for the synthesis of 1,3-dimethoxy-1,1,3,3-tetra-*n*-butyldistannoxane from *n*-Bu_2SnO and DMC, we studied the reactivity of **1** toward dimethyl carbonate (DMC) in methanol and in toluene solutions. In methanol, in the presence of stoichiometric amounts of DMC, overnight refluxing results in the total decomposition of **1**. Indeed, the infrared spectrum of the residual white powder reflects the exclusive presence of *n*-Bu_2SnO, the characteristic $\nu(CO_3)$ bands of **1** (1539 and 1373 cm^{-1}) having vanished totally. By contrast, in refluxing toluene, 1,3-dimethoxy-1,1,3,3-tetra-*n*-butyldistannoxane is generated quantitatively, the ^{119}Sn{^{1}H} as well as the ^{13}C{^{1}H} NMR spectra of the evaporated residue ($CDCl_3$, 298 K) displaying only the characteristic signals of {[*n*-$Bu_2(CH_3O)Sn]_2O$}$_2$ (^{119}Sn δ −174, −181 ppm, ^{13}C{^{1}H} δ (OCH_3) 51.6 ppm) [10]. The stoichiometry of the reaction between the oxocluster **1** and dimethyl carbonate, giving 1,3-dimethoxy-1,1,3,3-tetra-*n*-butyldistannoxane with release of CO_2, can be summarized according to the reaction equation:

$$(n\text{-}Bu_2SnO)_6[(n\text{-}Bu_2SnOCH_3)_2CO_3]_2 + 3\ (CH_3O)_2CO \rightarrow 5/2\ \{(n\text{-}Bu_2SnOCH_3)_2O\}_2 + 5\ CO_2$$

2.3.2. Reactivity of *PRE-1* with trifluoromethanesulfonic acid

Since single crystals of **PRE-1**, suitable for X-ray diffraction, could not be isolated, we have considered various reactions involving this compound, aiming to crystallise the resulting products, in order to make back tracing to the original structure of **PRE-1** possible. One of them involved reacting **PRE-1** with an excess of trifluoromethanesulfonic acid (TfOH) in acetonitrile, at room temperature. Thus, it is known that trifluoromethanesulfonic acid reacts with metal carbonates to form the corresponding trifluoromethanesulfonate derivatives under release of carbon dioxide and water [26]. Furthermore, several organotin(IV)

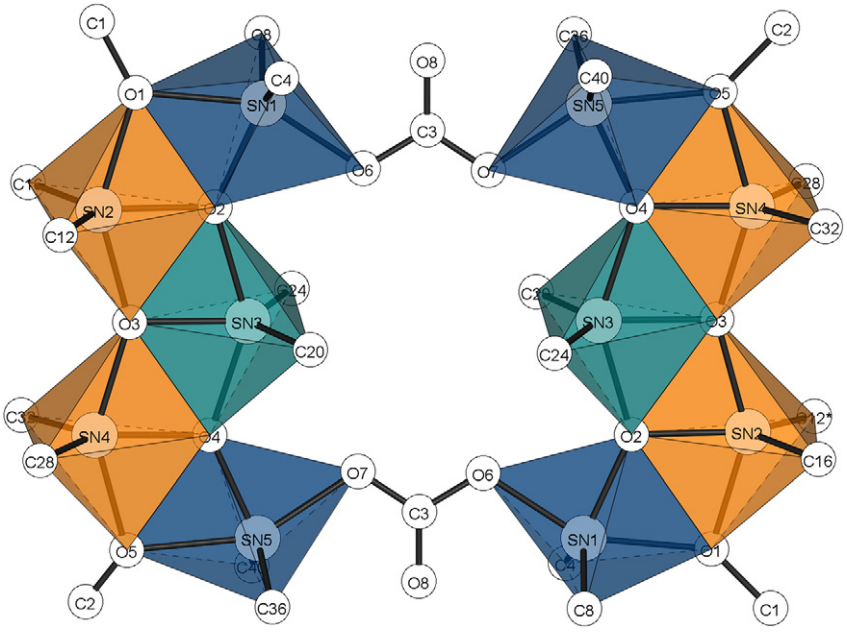

Fig. 6. A polyhedron coordination view of **1,** displaying the geometrical arrangement of the distorted trigonal bipyramidal tin atoms.

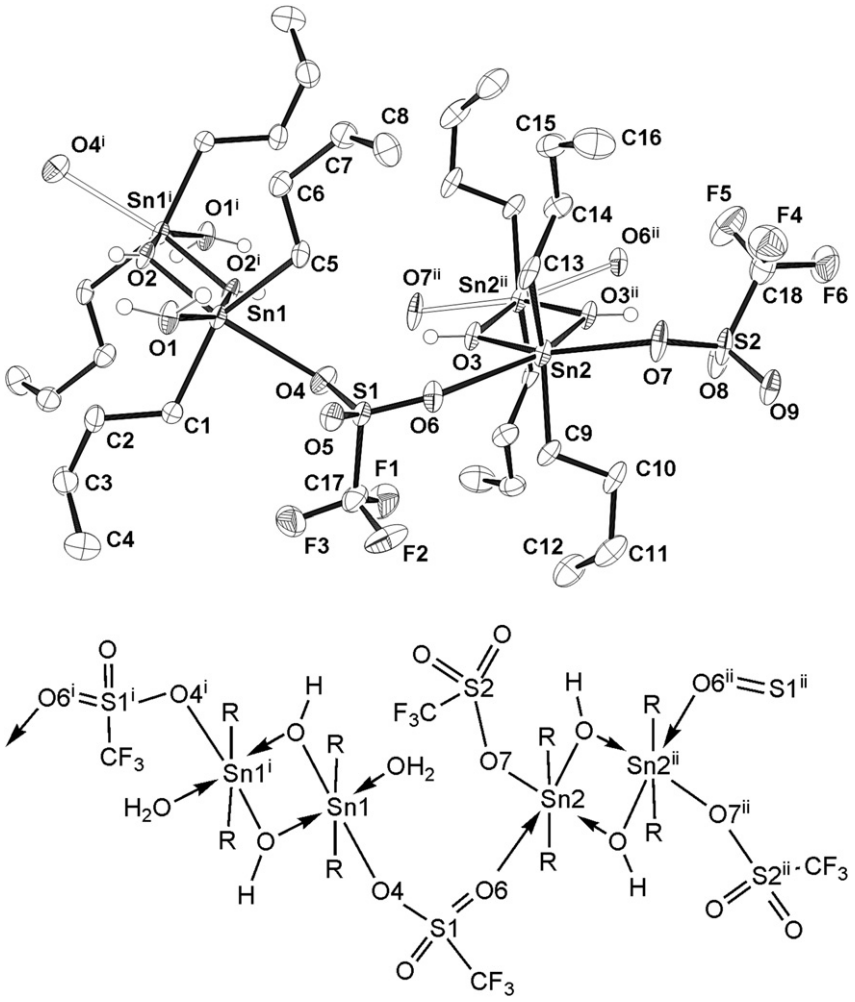

Fig. 7. Molecular scheme and ORTEP view of the molecular structure of $\{[n\text{-}Bu_2Sn(OH)(OTf)]_2[n\text{-}Bu_2Sn(OH)(OTf)(H_2O)]_2\}_n$ (**3**) with the atom-labelling scheme (50% probability ellipsoids). Open bonds indicate connection to atoms belonging to the rest of the polymer. Symmetry operations used to generate equivalent atoms: i = $-x$, $-y$, $-z$ and ii = $-x$, $1-y$, $2-z$.

trifluoromethanesulfonato compounds have been structurally elucidated by X-ray diffraction, revealing such compounds to be crystallisation friendly [27]. In the presence of trifluoromethanesulfonic acid, the starting white suspension of **PRE-1** gets progressively dissolved, leading finally to a completely clear solution. Colourless single crystals of **3**, suitable for X-ray diffraction, were obtained from dichloromethane/petroleum ether. The crystal unit cell consists of two independent dinuclear tin moieties with different compositions (see compound **3** in Scheme 1), constituting an infinite chain of cyclic dimeric μ_2-hydroxo di-*n*-butyltin(IV) triflate ($[n\text{-}Bu_2Sn(OH)(OTf)]_2$) units, each triflate bridging two such dimeric units as a bidentate, with the peculiar feature that the tin coordination number in each dimer is extended to 6, alternatively by one H_2O ligand per tin atom for the one dimer, and by one triflate ligand per tin atom for the neighbouring dimer. An ORTEP view of **3** is shown in Fig. 7, together with a drawing of the structure. All tin(IV) atoms are six-coordinated in a distorted octahedral geometry. The structure contains two types of trifluoromethanesulfonate ligands, *viz*. bridging and terminal. The uncoordinated O atoms of the terminal O_3SCF_3 ligand are involved in intra- and intermolecular hydrogen bonding interactions with bridging OH groups and coordinated water molecules. The structure found here for **3** is in agreement with the structure determined by Kim et al. [28] for the product of the reaction of di-*n*-butyltin oxide with an equimolar amount of trifluoromethanesulfonic acid. On the basis of the structure of **3**, and the basic structural motif proposed in Fig. 5(b), we suggest that upon reaction of **PRE-1** with triflic acid, each triflic acid unit protolyses a carbonate bridge to hydrogencarbonate and/or carbonic acid, that decompose(s) to water and carbon dioxide. The released pairs of $n\text{-}Bu_2SnO$ units are subsequently stabilized by cyclodimerization and protonation, and the four tin atoms are finally stabilized to six-coordination through ligation by bridging and terminal triflate ligands as well as water molecules. The generation of **3** from **PRE-1** and TfOH can be summarized according to the reaction equation (R = *n*-Bu):

$$2[(R_2SnO)_2\cdot CO_2] + 4TfOH + 2H_2O \rightarrow \{[R_2Sn(\mu_2\text{-}OH)(\text{inter-}\mu_2\text{-}OTf)(OH_2)]_2[R_2Sn(\mu_2\text{-}OH)(\mu_1\text{-}OTf)]_2\} + 2CO_2$$

3. Conclusion

Two efficient routes for the synthesis of the decakis(diorganotin (IV)) oxoclusters, $(n\text{-}Bu_2SnO)_6[(n\text{-}Bu_2SnOR)_2(CO_3)]_2$ (R = Me, **1**; R = Et, **2**) were reported. The sealed vial method based on the use of $n\text{-}Bu_2SnO$ as starting material is successful for the preparation of the ethoxy analogue **2.** Multinuclear solution 1D and 2D NMR

investigations, including solid-state measurements, enabled us to demonstrate that **1** and **2** display the same structural pattern, and that **1** displays identical solution and solid-state structures. Cluster **1** turns out to be an intermediate on the pathway of the reaction between *n*-Bu_2SnO and DMC to 1,3-dimethoxy-1,1,3,3-tetra-*n*-butyldistannoxane, which establishes the link between these three *n*-Bu_2SnO-based species. The solid-state NMR characterizations, supported by the X-ray determination of the structure of the triflate derivative **3** provides insight into the nature of **PRE-1**, the insoluble precursor of **1**, isolated from recycling experiments on **1**. The overall conclusion of the present work is that both clusters **1** and **2**, as well as the former's precursor, **PRE-1**, can be seen as powerful chemical capturers of carbon dioxide, at least when the latter is used in supercritical conditions. Both **1** and **PRE-1** turn out to be stable chemical CO_2 storage devices, that can however release CO_2 toward complex diorganotin compounds upon fine-tuning of their reactivity and reaction conditions.

4. Experimental

4.1. Spectroscopic measurements and instruments

The standard 1D NMR spectra were recorded at 295 K in $CDCl_3$ on a Bruker Avance 300 spectrometer (^1H = 300.13, ^{119}Sn = 111.91, and ^{13}C = 75.47 MHz). ^1H and ^{13}C chemical shifts (δ, ppm) were determined from the residual solvent signal ($C^1\underline{H}Cl_3$ δ 7.24, $^{13}\underline{C}DCl_3$ δ 77.0). $^{119}Sn\{^1H\}$ chemical shifts (δ, ppm) are reported toward $(CH_3)_4Sn$ used as an internal standard. All 2D spectra were recorded, using pulse sequences from the standard Bruker pulse library as described in Ref. [30], from sealed samples containing *ca.* 85 mg of cluster **1** or **2** in 0.5 mL of C_6D_6, at 303 K on a Bruker Avance II 500 spectrometer operating at (^1H = 500.13, ^{13}C = 125.77 and ^{119}Sn = 186.46 MHz). Chemical shifts were likewise determined from the residual solvent signal ($C_6D_5\underline{H}$ δ 7.15, $^{13}\underline{C}_6D_5H$ δ 128.0). (CP) MAS ^{117}Sn and ^{13}C solid-state spectra were recorded at 89.27 and 63.00 MHz, respectively, on a Bruker Avance 250 spectrometer, with a 4 mm MAS broad-band probe. Spinning frequencies were between 5 and 9 kHz for ^{117}Sn and 4 kHz for ^{13}C spectra. The chemical shift reference was set using (cyclo-$C_6H_{11})_4Sn$ (−97.35 ppm relative to $(CH_3)_4Sn$) and adamantine, respectively. The principle axis values of the ^{117}Sn chemical shielding tensors were fitted using the Herzfeld–Berger formalism, and the results obtained from the 'dmfit' program (Massiot D. *dmfit program*; available at http://crmht-europe.cnrs-orleans.fr). IR spectra were recorded on a Bruker Vector 22 equipped with a Specac Golden Gate™ ATR device. The ES mass spectrum was collected on a Bruker microOTOF-Q instrument using a methanol mobile phase. Elemental analyses were performed at the Institut de Chimie Moléculaire, Université de Bourgogne, Dijon and at the Service Central d'Analyses du CNRS, Solaize.

4.2. Syntheses

4.2.1. General

All manipulations were carried out by using standard Schlenk techniques [29] or sealed reaction vials. Toluene, methanol and ethanol (Carlo Erba, RPE grade) were dried and distilled under argon from CaH_2, $Mg(OCH_3)_2$, and $Mg(OCH_2CH_3)_2$, respectively. Carbon dioxide N45 TP purchased from Air Liquide was used without further purification. *n*-Bu_2SnO (purity ≥ 98%), dimethyl carbonate (purity ≥ 99%), and diethyl carbonate (purity ≥ 99%) were purchased from Acros Organics, Sigma–Aldrich, and Janssen, respectively, and were used without further purification.

4.2.2. Synthesis of (*n*-$Bu_2SnO)_6[(n$-$Bu_2SnOCH_3)_2(CO_3)]_2$(**1**)

An equimolar mixture of *n*-Bu_2SnO (2.652 g, 10.65 mmol) and dimethyl carbonate (0.958 g, 10.00 mmol) in toluene (25 mL) in the presence of methanol (0.2 mL) was heated in a sealed vial at 398 K. After *ca.* 30 min, the suspension turned to a clear solution and heating was continued for another 40 min. After cooling down to room temperature, filtration and removal of the volatiles under vacuum, a white sticky solid was obtained. Several washings with aliquots of methanol (5 mL) led to a fine white powder characterized as compound **1**. Yield: 2.491 g (86%). NMR data are given in Tables 1 and 3. IR (neat): ν(CH) 2956, 2921, 2871, 2855 cm^{-1},ν(CHmethoxy) 2801 cm^{-1}, $\nu(CO_3)$ 1539 (s), 1373 (vs) cm^{-1}. Elemental analysis (%): Found: C, 38.98; H, 7.09; Sn, 45.30, calcd for $C_{86}H_{192}O_{16}Sn_{10}$ (2669.56): C, 38.69; H, 7.25; Sn, 44.47.

4.2.3. Synthesis of (*n*-$Bu_2SnO)_6[(n$-$Bu_2SnOCH_2CH_3)_2(CO_3)]_2$(**2**)

Compound **2** was prepared similarly to **1**, from an equimolar mixture of *n*-Bu_2SnO (2.500 g, 10.00 mmol) and diethyl carbonate (1.180 g, 10.00 mmol) in toluene (25 mL) in the presence of ethanol (0.2 mL). The mixture was stirred at 398 K for 90 min in a sealed vial. After cooling of the clear solution, the solvent was evaporated under vacuum. The tin-based residue was then washed with ethanol. Yield in compound **2**: 1.506 g (55%). NMR data are given in Table 2. IR (neat): ν (CH) 2954, 2921, 2869, 2854 cm^{-1}, $\nu(CO_3)$ 1535 (s), 1374 (vs) cm^{-1}. Elemental analysis (%): Found: C, 39.21; H, 7.79; Sn, 44.70, calcd for $C_{90}H_{200}O_{16}Sn_{10}$ (2725.64): C, 39.66; H, 7.40; Sn, 43.55.

4.2.4. Synthesis of ***PRE-1***

A volume of 40 mL of toluene was added to 2.515 g of *n*-Bu_2SnO (10 mmol based on tin) in a 120 cm^3 stainless steel batch autoclave. Subsequently, CO_2 was introduced at 4 MPa, at room temperature. The autoclave was heated up to 383 K, as controlled by an internal thermocouple, and the pressure was adjusted to the desired value (11 MPa) by a high-pressure CO_2 pump (Top Industrie S.A., France). After 15 h of reaction under magnetic stirring, the autoclave was cooled down to 273 K, depressurised and the suspension phase transferred to a Schlenk tube. After filtration, **PRE-1** was collected as an amorphous white powder. Yield: 0.600 g. Solid-state $^{117}Sn\{^1H\}$ RMN data are provided in Table 3. IR (neat): ν (CH) 2957, 2925, 2858 cm^{-1}, $\nu(CO_3)$ 1505 (br), 1371 (vs) cm^{-1}. Elemental analysis (%): found: C, 38.76; H, 7.12; Sn 44.93, Calculated for the proposed structure $((C_4H_9)_2Sn)_2OCO_3$ (541.89) [21]: C, 37.68; H, 6.70; Sn 43.81.

4.2.5. Synthesis of {[*n*-$Bu_2Sn(OH)(OTf)]_2$[*n*-$Bu_2Sn(OH)(OTf)(H_2O)]_2\}_n$ (**3**)

A suspension of **PRE-1** (0.250 g) and TfOH (0.057 g, 0.38 mmol) in acetonitrile (20 mL) was stirred at room temperature. After one night, an additional amount of TfOH (0.057 g, 0.38 mmol) is added to the suspension, quickly giving a clear solution. After filtration and evaporation, the residue is dissolved in a mixture of dichloromethane/petroleum ether, giving rise after one week to single crystals suitable for X-ray diffraction and characterized as the complex **3** described previously [28].

4.3. Crystal structure determination for **3**

Colourless prismatic single crystals of {[*n*-$Bu_2Sn(OH)(OTf)]_2$[*n*-$Bu_2Sn(OH)(OTf)(H_2O)]_2$} were grown from a mixture of dichloromethane/petroleum ether at room temperature. Diffraction data were collected from a suitable crystal (0.22 × 0.22 × 0.25 mm) on a Nonius Kappa CCD (Mo Kα radiation, λ = 0.71073 Å). The structure was solved using a direct method (SIR 92) [31] and refined with full-matrix least-squares methods based on F^2 (SHELX-97) [32] with the

aid of the WINGX program [33]. Except for the minor components of the disordered *n*-butyl groups, all non-hydrogen atoms were anisotropically refined. Hydrogen atoms were included in their calculated positions or found in the final difference Fourier maps and refined with a riding model. Two *n*-butyl groups were found to be disordered over two positions (occupations factors: converged to 0.71:0.29 for C9–C12 and 0.68:0.32 for C13–C16).

Crystal data. $C_{36}H_{80}F_{12}Sn_4O_{18}S_4$, $M = 1632$ g mol^{-1}, triclinic, $a = 9.7725(2)$ Å, $b = 11.3065(3)$ Å, $c = 14.5199(4)$ Å, $\alpha = 82.223(1)^\circ$, $\beta = 72.021(1)^\circ$, $\gamma = 82.949(1)^\circ$, $V = 1506.38$ Å^3; $T = 115(2)$ K, space group $P-1$, $Z = 1$, μ(Mo Kα) = 1.87 mm^{-1}, 11 414 collected reflections, 6916 unique ($R_{int} = 0.019$) which were used in all calculations. The final $R(F)$ and $wR(F^2)$ were 0.041 and 0.078 (all data), respectively; number of parameters = 369.

Acknowledgements

We are grateful for financial support to this work from the Centre National de la Recherche Scientifique and from the Ministère de la Recherche for post-doctoral and doctoral grants (RL, SC). The financial support by the fund of Scientific Research Flanders (Belgium) (FWO) (Grant G.0469.06) and the Research Council (Onderzoeksraad) of the Vrije Universiteit Brussel (Concerted Research Action, Grant GOA31) to RW and MB is gratefully acknowledged.

References

[1] (a) V. Chandrasekhar, K. Gopal, P. Thilagar, Acc. Chem. Res. 40 (2007) 420;
(b) V. Chandrasekhar, K. Gopal, P. Sasikumar, R. Thirumoorthi, Coor. Chem. Rev. 249 (2005) 1745;
(c) V. Chandrasekhar, S. Nagendran, V. Baskar, Coord. Chem. Rev. 235 (2002) 1.
[2] (a) S.P. Narula, S. Kaur, R. Shankar, S. Verma, P. Venugopalan, S.K. Sharma, Inorg. Chem. 38 (1999) 4777;
(b) R. García-Zarracino, J. Ramos-Quiñones, H. Höpfl, Inorg. Chem. 42 (2003) 3835;
(c) R. García-Zarracino, H. Höpfl, J. Am. Chem. Soc. 127 (2005) 3120;
(d) V. Chandrasekhar, R. Thirumoorthi, R. Azhakar, Organometallics 26 (2007) 26.
[3] T. Sato, Y. Wakahara, J. Otera, H. Nozaki, Tetrahedron 47 (1991) 9773.
[4] T. Sato, Y. Wakahara, J. Otera, H. Nozaki, Tetrahedron Lett. 31 (1990) 1581.
[5] K. Sakamoto, Y. Hamada, H. Akashi, A. Orita, J. Otera, Organometallics 18 (1999) 3555.
[6] (a) J. Otera, Acc. Chem. Res. 37 (2004) 288;
(b) H. Lee, J.Y. Bae, O.-S. Kwon, S.J. Kim, S.D. Lee, H.S. Kim, J. Organomet. Chem. 689 (2004) 271.
[7] C.J. Evans, S. Karpel, Organotin Compounds in Modern Technology. Elsevier Science Publishers, Amsterdam, 1985.
[8] (a) J. Kizlink, I. Pastucha, Collect. Czech. Chem. Commun. 6 (1995) 687;
(b) J.-C. Choi, T. Sakakura, T. Sako, J. Am. Chem. Soc. 121 (1999) 3793;
(c) N.S. Isaacs, B. O'Sullivan, C. Verhaelen, Tetrahedron 55 (1999) 11949;
(d) T. Sakakura, J.-C. Choi, Y. Saito, T. Masuda, T. Sako, T. Oriyama, J. Org. Chem. 64 (1999) 4506.
[9] D. Ballivet-Tkatchenko, O. Douteau, S. Stutzmann, Organometallics 19 (2000) 4563.
[10] D. Ballivet-Tkatchenko, T. Jerphagnon, R. Ligabue, L. Plasseraud, D. Poinsot, Appl. Catal. A: General 255 (2003) 93.
[11] D. Ballivet-Tkatchenko, H. Chermette, L. Plasseraud, O. Walter, Dalton Trans. (2006) 5167.
[12] D. Ballivet-Tkatchenko, R. Burgat, S. Chambrey, L. Plasseraud, P. Richard, J. Organomet. Chem. 691 (2006) 1498.
[13] D. Ballivet-Tkatchenko, S. Chambrey, R. Keiski, R.A. Ligabue, L. Plasseraud, P. Richard, H. Turunen, Catal. Today 115 (2006) 80.
[14] R.K. Harris, A. Sebald, J. Organomet. Chem. 331 (1987) C9.
[15] I. Omae, Organotin Chemsitry, (J. Organomet. Chem. Library vol. 21), Elsevier, Amsterdam (1989).
[16] A.G. Davies, D.C. Kleinschmidt, P.R. Palan, S.C. Vasishta, J. Chem. Soc. (C) (1971) 3972.
[17] A.G. Davies, P.G. Harrison, J. Chem. Soc. (C) (1967) 298.
[18] C. Vatsa, V.K. Jain, T.K. Das, J. Organomet. Chem. 418 (1991) 329.
[19] D. Ballivet-Tkatchenko, unpublished results.
[20] P.J. Smith, R. Hill, J. Organomet. Chem. 252 (1983) 149.
[21] R.G. Goel, H.S. Prasad, G.M. Bancroft, T.K. Sham, Can. J. Chem. 54 (1976) 711.
[22] B. Wrackmeyer, Annual Reports on NMR Spectroscopy 16 (1985), p. 73.
[23] M. Kemmer, M. Biesemans, M. Gielen, J.C. Martins, V. Gramlich, R. Willem, Chem. Eur. J. 7 (2001) 4686.
[24] M. Biesemans, J.C. Martins, R. Willem, A. Lyčka, A. Růžička, J. Holeček, Magn. Res. Chem. 40 (2002) 65.
[25] The solid-state ^{117}Sn rather than the ^{119}Sn NMR spectrum was recorded because of local radio interferences.
[26] R.D. Howells, J.D. McCown, Chem. Rev. 77 (1977) 69.
[27] J. Beckmann, Appl. Organomet. Chem. 19 (2005) 494.
[28] H. Lee, J.Y. Bae, O.-S. Kwon, S.J. Kim, S.D. Lee, H.S. Kim, J. Organomet. Chem. 689 (2004) 1816.
[29] D.F. Shriver, The Manipulation of Air-Sensitive Compounds. McGraw-Hill, New York, 1986.
[30] S. Berger, S. Braun, 200 and more NMR experiments, Wiley VCH (2004), and references cited herein.
[31] A. Altomare, G. Cascarano, C. Giacovazzo, A. Guagliardi, J. Appl. Crystallogr. 26 (1993) 343.
[32] G.M. Sheldrick, Shelx-97 (includes Shelxs-97 and Shelxl-97), Release 97-2, Programs for Crystal Structure Analysis. University of Göttingen, Göttingen, Germany, 1998.
[33] L.J. Farrugia, J. Appl. Crystallogr. 32 (1999) 837.